

Utilizing MRI Radiomics and Clinical Features to Predict Severe Acute Pancreatitis in Patients with Metabolic Syndrome

Yuan Wang*, Xiyao Wan*, Yawen Zhang, Ziyang Liu, Ziyi Liu, Mengyue Tang, Xiaohua Huang

Department of Radiology, Affiliated Hospital of North Sichuan Medical College, Nanchong, Sichuan, 637000, People's Republic of China

*These authors contributed equally to this work

Correspondence: Xiaohua Huang, Affiliated Hospital of North Sichuan Medical College, Department of Radiology, Nanchong, Sichuan, 637000, People's Republic of China, Tel +86150-8279-7553, Email 15082797553@163.com

Background: Early identification of severe acute pancreatitis (SAP) in patients with metabolic syndrome (MetS) is crucial for improving prognosis and guiding timely intervention. Conventional scoring systems such as the bedside index for severity in acute pancreatitis (BISAP) and magnetic resonance severity index (MRSI) show limited accuracy for early prediction. MRI-based radiomics offers a noninvasive approach to quantify subtle image features that may reflect underlying disease heterogeneity. Integrating radiomics with clinical indicators may enhance prediction of SAP progression in MetS patients.

Purpose: To develop and validate a predictive model combining MRI T2WI radiomics and clinical features to predict SAP occurrence in MetS patients.

Patients and Methods: This retrospective study included 188 patients with acute pancreatitis (AP) and MetS, classified into severe (31 patients) and non-severe (157 patients) groups according to the 2012 revised Atlanta consensus. Regions of interest were delineated using 3D Slicer, and radiomics features were extracted via PyRadiomics. Features were normalized and selected using select K-best and least absolute shrinkage and selection operator (LASSO). A random forest classifier constructed the radiomics model, while binary logistic regression identified independent clinical predictors to form a combined model. Model performance and clinical utility were evaluated using the area under the curve (AUC), the DeLong test, and decision curve analysis (DCA).

Results: Seven radiomics features were selected following dimensionality reduction. Binary logistic regression identified length of hospital stay and serum calcium as independent clinical risk factors. The combined model achieved AUCs of 0.97 and 0.979 in training and test sets, respectively, outperforming the clinical, radiomics, BISAP, and MRSI models.

Conclusion: The combined model integrating MRI T2WI radiomics with clinical features provides robust and clinically valuable prediction of SAP in MetS patients, supporting its potential value for early clinical intervention.

Keywords: acute pancreatitis, severity, metabolic syndrome, radiomics, magnetic resonance imaging

Introduction

Acute pancreatitis (AP) is among the most prevalent acute gastrointestinal disorders, with a global incidence of 30–40 cases per 100,000 individuals. The typical presentation is severe abdominal pain, fever, and dyspepsia.^{1,2} Although most cases resolve rapidly, approximately 20% of patients develop severe AP (SAP), which carries a mortality rate of 20%–40%.^{3,4} Dyslipidemia, hyperglycemia, and elevated body mass index (BMI) values are associated with risk of progression to SAP.^{5–7} Metabolic syndrome (MetS), defined by central obesity, insulin resistance, hypertension, and dyslipidemia, is significantly linked to both AP severity and mortality.^{8,9} MetS contributes to AP development and progression through mechanisms such as chronic low-grade inflammation, lipid metabolism disorders, and microcirculatory dysfunction. These processes facilitate the secretion of inflammatory cytokines and promote free fatty acids (FFAs) accumulation, aggravating the pancreatic injury and facilitating the transition to severe disease.^{10,11} As the prevalence of MetS continues to increase, its presence at admission has

become a major contributor to the increasing incidence of SAP.⁹ Timely and accurate prediction of SAP in MetS cases is essential for guiding clinical decision-making and improving prognostic outcomes.

Several scoring systems are currently employed to assess AP severity, including the bedside index for severity in AP (BISAP) and the magnetic resonance severity index (MRSI).^{12,13} BISAP is a rapid, bedside scoring tool designed to identify high-risk patients; however, it has limited sensitivity for predicting SAP and does not fully reflect pancreatic pathological changes.¹⁴ Enabling high resolution of soft tissues, MRI is a preferred imaging modality for evaluating pancreatitis and its local complications. T2WI offers higher sensitivity than CT in detecting fluid collections and subtle peripancreatic inflammation.^{15,16} Although MRSI has demonstrated value in assessing AP severity, particularly in the study by Tang et al, early AP may present with minimal morphological changes on MRI, potentially resulting in an underestimation of disease severity and limiting its early diagnostic utility.¹³

Radiomics enables the extraction of numerous quantitative features from medical images, revealing tissue heterogeneity not discernible by visual inspection.¹⁷ In early AP, radiomics features can capture subtle variations in pancreatic parenchyma that correspond to differences in disease severity. By quantifying spatial and textural characteristics—such as gray-level nonuniformity, local intensity variations, and multi-scale edge details—radiomics can objectively reflect pancreatic edema, necrosis, and peripancreatic inflammation that are often invisible to traditional scoring systems like BISAP or MRSI.¹⁷ This quantitative approach transforms subjective image interpretation into reproducible analysis, enabling earlier and more precise assessment of tissue injury. Previous studies have shown promising results in predicting AP severity using radiomics.^{15,16} However, most investigations have focused on general AP populations, with limited attention to SAP prediction in the context of MetS. Current studies examining the relationship between MetS and AP severity have primarily evaluated differences in clinical features.⁸ This study aims to integrate radiomics features derived from MRI with clinical parameters to construct a model for predicting SAP in patients with MetS, thereby improving the identification of cases with elevated risk, enabling timely intervention to reduce SAP-associated mortality.

Materials and Methods

Study Population

This retrospective study included patients diagnosed with AP in the context of MetS between June 2021 and July 2024. The study protocol was approved by the Medical Ethics Committee of Affiliated of North Sichuan Medical College, and due to its retrospective design, the requirement for informed consent was waived (Approval Number: 2024ER94-1). Inclusion criteria were as follows: (1) an AP diagnosis according to the 2012 revised Atlanta Consensus;¹⁸ (2) diagnosis of MetS,¹⁹ with BMI ≥ 28 kg/m² adopted as a surrogate for waist circumference (not routinely measured in this retrospective analysis) to define obesity;²⁰ and (3) conventional MRI performed within 7 days of admission. Cases were excluded if they: (1) were aged <18 years; (2) had acute exacerbation of chronic pancreatitis; (3) had benign or malignant pancreatic tumors; and (4) had poor MRI image quality.

Overall, 188 cases with AP and MetS were enrolled based on hospitalization and follow-up records. According to the 2012 revised Atlanta Consensus, patients were stratified by severity into mild AP (MAP), moderately severe AP (MSAP), and SAP. The MAP and MSAP cases represented non-severe AP (NSAP) group, whereas SAP cases constituted the SAP group. Patients were randomly allocated in a 7:3 ratio into a training set (131 patients: 109 NSAP, 22 SAP) and a test set (57 patients: 48 NSAP, 9 SAP). The recruitment process is depicted in [Figure 1](#).

Clinical Data

Clinical variables were obtained, including demographic and laboratory parameters: sex, age, etiology, recurrence, hypertension, diabetes, hyperlipidemia, fatty liver, BMI, length of hospital stay, systemic inflammatory response syndrome, pleural effusion, peritoneal effusion, blood glucose, triglycerides, C-reactive protein (CRP), serum calcium, low-density lipoprotein cholesterol (LDL-C), and high-density lipoprotein cholesterol (HDL-C), among others.

MRI Scanning Protocol

All enrolled patients underwent upper abdominal plain MRI using a 16-channel body phased-array coil system (uMR790, United Imaging Healthcare, Shanghai, China). Patients fasted, abstained from water intake, and underwent respiratory training

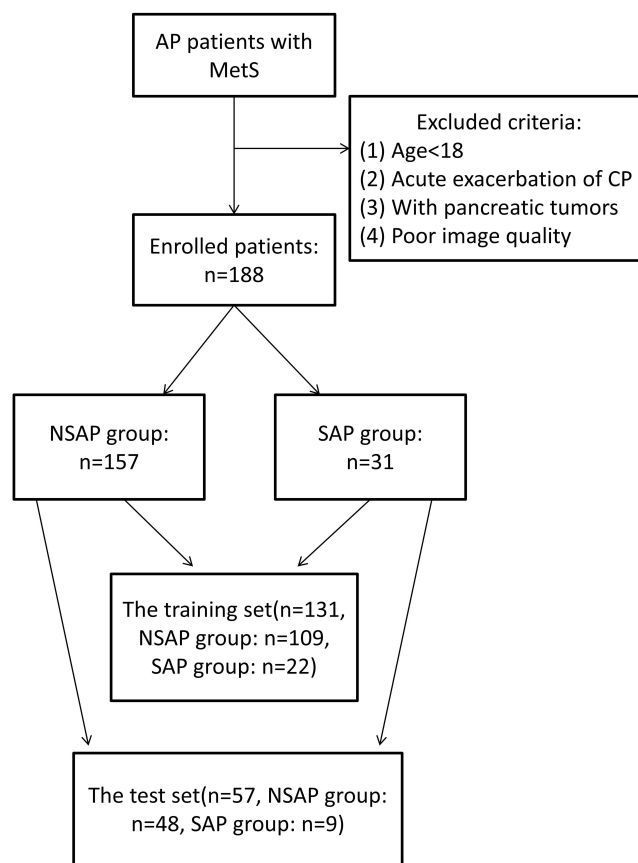


Figure 1 Flow chart of patient recruitment in this study.

before scanning. During imaging, patients were positioned supine with their head in the entry position. Respiratory gating was synchronized with the point of maximum abdominal motion, and the scanning field encompassed the entire upper abdomen. A transverse fast spin-echo sequence employing artificial intelligence-assisted compressed sensing technology was used. The parameters used for scanning comprised: repetition time (TR) 8000 ms, echo time (TE) 116 ms, field of view (FOV) 38 cm × 30 cm, slice thickness 5.0 mm, interslice gap 2.0 mm, and matrix size 256×171.

Image Analysis and Feature Selection

T2-weighted MRI images were analyzed in 3D Slicer (version 5.2.2; <https://www.slicer.org/>). Regions of interest (ROIs) were delineated manually by a radiologist with five years of specialization in abdominal imaging, using layer-by-layer contouring along the pancreatic boundary to encompass both parenchymal and necrotic regions. This manual segmentation ensured accurate identification of subtle morphological variations in the pancreas. To standardize image data before radiomics analysis, the resampling of the images was carried out to an isotropic voxel size of 1 × 1×1 mm. Laplacian of Gaussian filters with sigma values of 0.5, 1.0, 1.5, and 2.0 were applied to extract multi-scale texture features and grayscale intensity values were discretized using a fixed bin width of 25 to minimize noise.

A total of 1223 features were extracted using the “PyRadiomics” package. To assess inter-observer consistency, ROIs from 63 randomly selected cases (one-third of the total patients) were independently delineated by another experienced abdominal radiologist blinded to clinical data. Inter-observer agreement was estimated using the intraclass correlation coefficient (ICC), and features with ICC > 0.80 were considered reproducible. Feature standardization was performed using z-score normalization. Feature selection was then conducted using the select K-best method followed by the least absolute shrinkage and selection operator (LASSO) algorithm. The workflow of this study is shown in Figure 2.

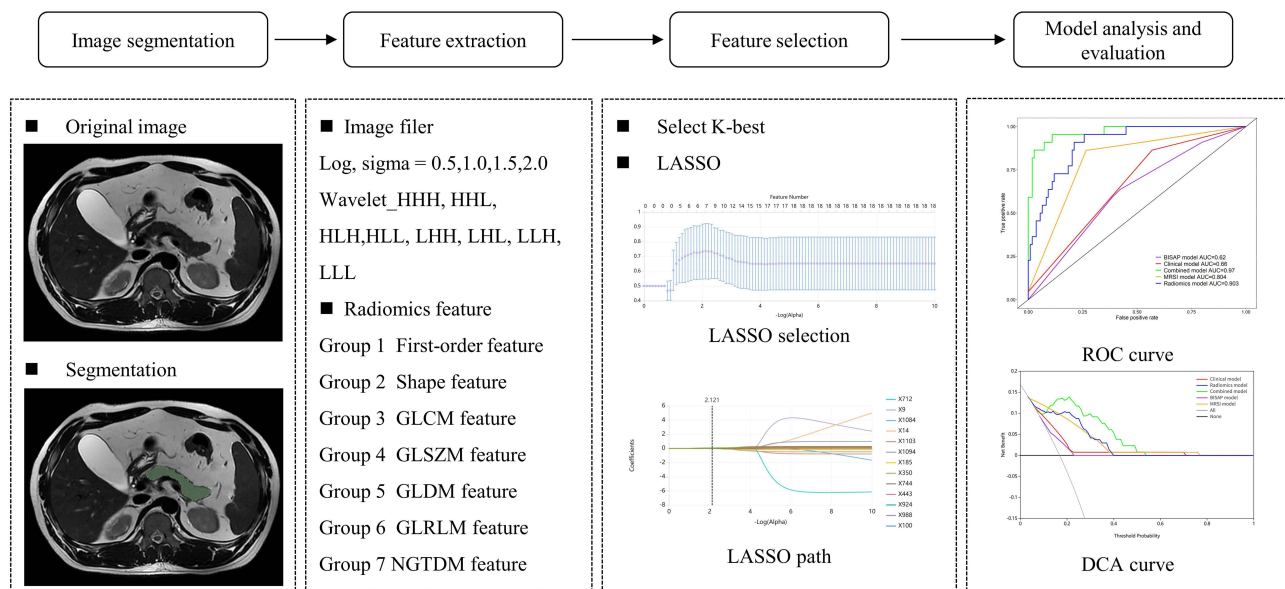


Figure 2 The radiomics workflow of this study.

Model Construction and Evaluation

A random forest classifier was utilized for the construction of a clinical model using the risk factors identified by binary logistic regression, a radiomics model using selected radiomics features, and a combined model integrating both clinical and radiomics features. The random forest was implemented with 100 trees, a maximum tree depth of 2, and the Gini impurity criterion for node splitting. BISAP and MRSI scores were calculated for each patient, and corresponding BISAP and MRSI models were developed accordingly. Model performance for predicting SAP in the context of MetS was evaluated using the area under the receiver operating characteristic (ROC) curve (AUC), specificity, sensitivity, and accuracy. The DeLong test was employed to compare predictive performance among models. DCA was conducted to assess the clinical utility. Radiomics feature selection and model construction were undertaken with R software (version 4.3.2) and the United Imaging uAI Research Portal (version 1.6).

Statistical Analysis

Clinical data were analyzed using SPSS 27.0. For comparing continuous variables with normal distribution, independent samples *t* test was used, with results presented as mean \pm standard deviation. Non-normally distributed continuous data were compared using the Mann–Whitney *U*-test and written as median (interquartile range). Categorical variables were analyzed using the χ^2 -test or Fisher's exact test, and findings are shown as counts (percentages). $P < 0.05$ was considered statistically significant.

Results

Clinical Data Analysis

General characteristics and laboratory parameters of the enrolled patients are presented in Table 1. Among the 188 individuals, 90 (47.9%) were diagnosed with MAP, 67 (35.6%) with MSAP, and 31 (16.5%) with SAP. Significant differences between the groups were found in terms of hospital stay, pleural effusion, peritoneal effusion, serum calcium, HDL-C, LDL-C, CRP, and amylase levels. No statistically significant differences were found for the remaining clinical variables. Binary logistic regression analysis identified length of hospital stay and serum calcium as independent predictors of SAP in patients with MetS, with odds ratios of 1.205 (95% CI: 1.100–1.321) and 0.007 (95% CI: 0.000–0.131), respectively ($P < 0.05$).

Table 1 Patient Characteristics

| | NSAP (n=157) | SAP (n=31) | P value |
|--|---------------------|----------------------|---------------------|
| General data | | | |
| Age, years | 46 (36–54) | 45 (41–55) | 0.544 ^a |
| Male | 96 (61.2%) | 17 (54.8%) | 0.512 ^c |
| BMI, kg/m ² | 27.3±3.3 | 26.8±4.1 | 0.469 ^b |
| Aetiology | | | 0.770 ^c |
| Biliary | 42 (26.8%) | 7 (22.5%) | |
| Hypertriglyceridaemia | 98 (62.4%) | 20 (64.5%) | |
| Alcohol | 5 (3.2%) | 2 (6.5%) | |
| Other | 12 (7.6%) | 2 (6.5%) | |
| Hypertension | 36 (22.9%) | 9 (29.0%) | 0.467 ^c |
| Diabetes | 47 (29.9%) | 13 (41.9%) | 0.190 ^c |
| Hyperlipidaemia | 113 (72.0%) | 23 (74.2%) | 0.801 ^c |
| Fatty liver | 100 (63.7%) | 19 (61.3%) | 0.800 ^c |
| Length of hospital stay, days | 10 (8–12) | 16 (11–22) | <0.001 ^a |
| Pleural effusion | 103 (65.6%) | 28 (90.3%) | 0.006 ^c |
| Ascites | 38 (24.2%) | 17 (54.8%) | 0.001 ^c |
| SIRS | 64 (40.8%) | 16 (51.6%) | 0.264 ^c |
| Recurrence | 68 (43.3%) | 17 (54.8%) | 0.239 ^c |
| Smoking | 54 (34.4%) | 10 (32.3%) | 0.819 ^c |
| Alcohol consumption | 74 (47.1%) | 16 (51.6%) | 0.648 ^c |
| Laboratory data | | | |
| Amylase, U/L | 187 (69–398) | 281 (112–1187) | 0.034 ^a |
| Lipase, U/L | 304 (113–1047.5) | 548 (141–1787) | 0.066 ^a |
| Calcium, mmol/L | 2.28 (2.19–2.36) | 2.11 (1.99–2.23) | <0.001 ^a |
| Triglyceride, mmol/L | 4.62 (2.43–11.52) | 4.48 (2.03–13.21) | 0.887 ^a |
| HDL-C, mmol/L | 0.81 (0.65–1.01) | 0.67 (0.47–0.91) | 0.037 ^a |
| LDL-C, mmol/L | 2.43 (1.64–3.10) | 1.58 (1.03–2.95) | 0.042 ^a |
| Total cholesterol, mmol/L | 5.44 (4.59–6.81) | 5.72 (3.94–8.06) | 0.954 ^a |
| CRP, mg/L | 34.5 (7.70–126.30) | 123.0 (17.90–196.10) | 0.011 ^a |
| Glucose, mmol/L | 7.63 (6.38–10.88) | 8.67 (7.37–12.47) | 0.084 ^a |
| WBC count, ×10 ⁹ /L | 12.9±4.3 | 13.6±5.6 | 0.418 ^b |
| Neutrophile granulocyte, ×10 ⁹ /L | 10.65±4.15 | 11.70±5.35 | 0.222 ^b |

Notes: ^aData are expressed as median (interquartile range). Group comparisons were performed using the Mann–Whitney *U*-test. ^bData are expressed as mean ± standard deviation. Group comparisons were performed using the independent samples *t* test. ^cData are expressed as number (%). Group comparisons were performed using the χ^2 -test or Fisher's exact test, as appropriate. *P* < 0.05 was considered statistically significant.

Abbreviations: NSAP, non-severe acute pancreatitis; SAP, severe acute pancreatitis; BMI, body mass index; SIRS, systemic inflammatory response syndrome; HDL-C, high density lipoprotein cholesterol; LDL-C, low density lipoprotein cholesterol; CRP, C-reactive protein; WBC, white blood cell.

Feature Selection

From the T2WI, a total of 1223 radiomics features were extracted. Following inter-observer reliability screening with an ICC threshold > 0.80 , 986 features were retained (Figure 3). Sequential application of the select K-best method and the LASSO algorithm yielded seven optimal features (Figure 4A and B). These included one second-order feature, four higher-order features, and two wavelet-transformed higher-order features (Table 2).

Model Performance Evaluation

Table 3 summarizes the BISAP and MRSI scores in the SAP and NSAP groups. Both BISAP and MRSI scores were significantly elevated in the SAP group. ROC curves were utilized to compare the predictive performance of five models constructed using a random forest classifier (Figure 4C and D). In the training set, the AUCs for the combined, radiomics, MRSI, BISAP, and clinical models were 0.97, 0.903, 0.804, 0.62, and 0.66, respectively. In the test set, these values were 0.979, 0.831, 0.731, 0.668, and 0.743, respectively. In the training set, the specificity, accuracy, and sensitivity of the combined model were 0.972, 0.954, and 0.864, respectively, whereas in the test set, these values were 0.854, 0.877, and 0.857, respectively. The remaining model metrics are shown in Table 4.

The DeLong test demonstrated that the combined model outperformed the radiomics model (training set: $P = 0.003$; test set: $P = 0.008$), clinical model (training set: $P < 0.001$; test set: $P = 0.001$), MRSI model (training set: $P < 0.001$; test set: $P = 0.018$), and BISAP model (training set: $P < 0.001$; test set: $P < 0.001$). In the training set, both the radiomics model and MRSI models demonstrated better predictive performance than the clinical model ($P < 0.001$, $P = 0.034$) and BISAP model ($P < 0.001$, $P = 0.015$); however, the radiomics model and MRSI models did not differ significantly ($P = 0.068$). In the test set,

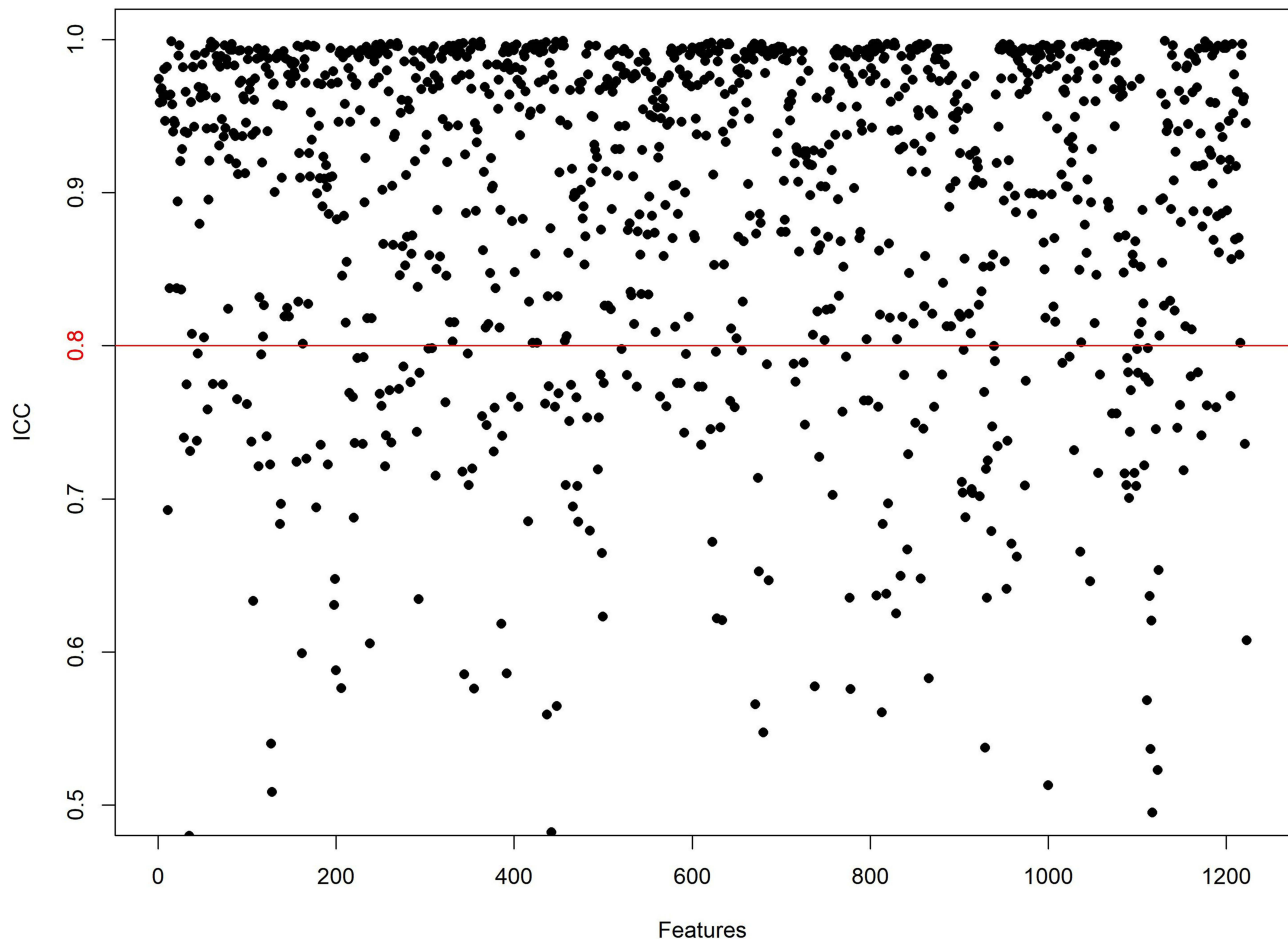


Figure 3 Intraclass consistency test. Values above the red line indicate ICC > 0.80 , signifying high reliability of the radiomics features extracted by the two observers.

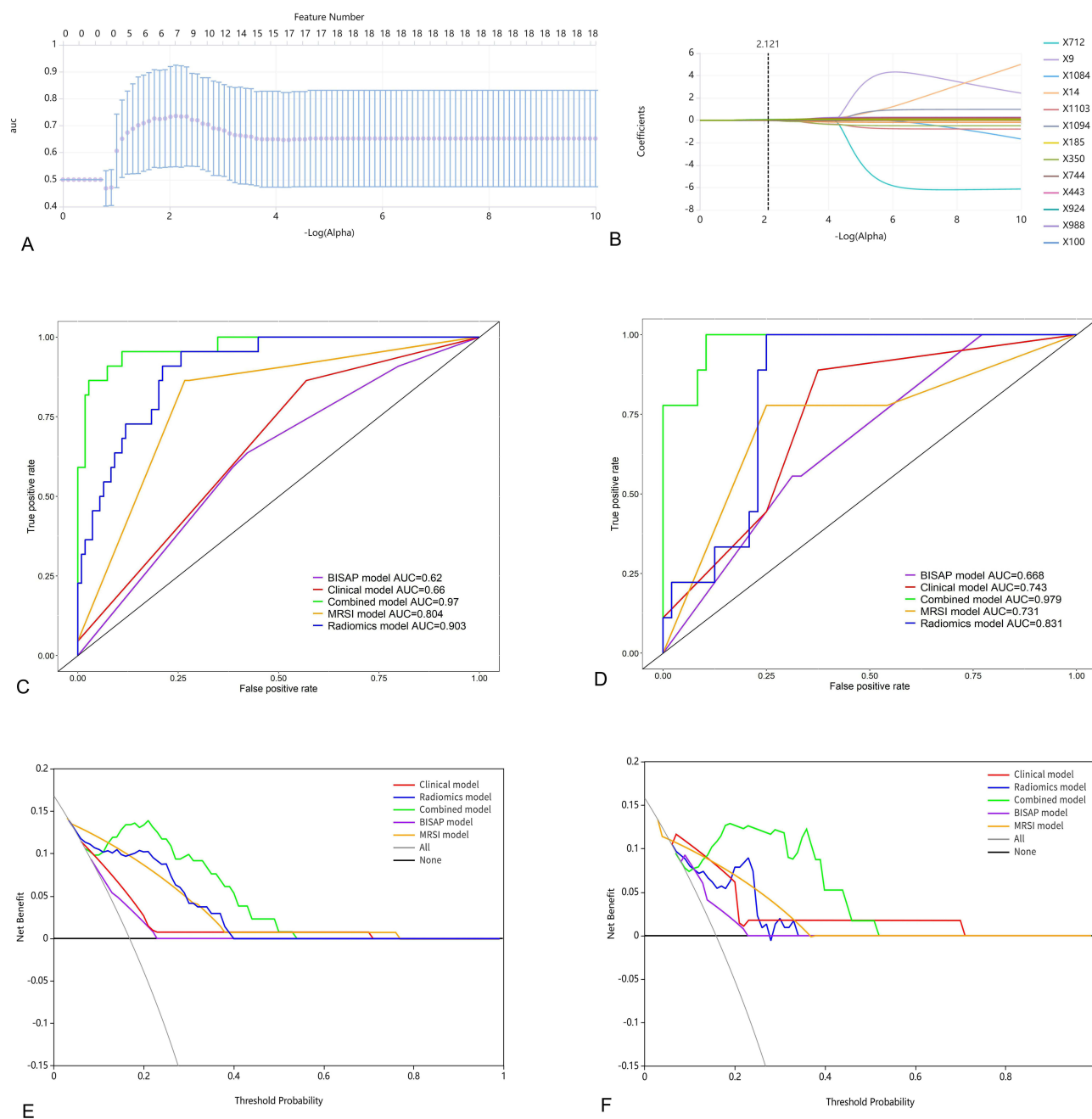


Figure 4 Feature selection and model performance for predicting severe acute pancreatitis (SAP) in patients with metabolic syndrome (MetS). Feature selection using the least absolute shrinkage and selection operator (LASSO). **(A)** Feature selection; **(B)** Curve of coefficient variation. The receiver operating characteristic (ROC) curve for the models. **(C)** Training set; **(D)** Test set. Decision curve analysis of the models. **(E)** Training set; **(F)** Test set.

no marked differences were observed among the remaining models ($P > 0.05$). DCA confirmed that the combined model offered the most significant net clinical benefit relative to the other models (Figure 4E and F).

Discussion

This study established a combined model integrating clinical and radiomics characteristics to enable individualized prediction of AP severity in MetS cases. Compared to the standalone clinical, radiomics, BISAP, and MRSI models, the combined model achieved better predictive performance, with AUC values of 0.97 and 0.979 in the training and test sets, respectively. These findings indicate that integrating radiomics and clinical features may serve as a valuable approach for

Table 2 Selected Radiomics Features and Their Coefficients

| Feature | Coefficient |
|--|---------------|
| Original_gldm_LargeDependenceHighGrayLevelEmphasis | 0.04563457 |
| Original_glrIm_LongRunHighGrayLevelEmphasis | 0.0185434856 |
| Original_glszm_ZoneEntropy | 0.0178584438 |
| Log-sigma-0-5-mm-3D_glszm_LargeAreaHighGrayLevelEmphasis | 0.0420167334 |
| log-sigma-1-5-mm-3D_glrIm_GrayLevelNonUniformity | -0.0131694516 |
| Wavelet-LHH_ngtdm_Busyness | 0.05581711 |
| Wavelet-HLH_glszm_GrayLevelNonUniformity | 0.07429575 |
| 0.167938933 | Constant |

Abbreviations: GLDM, gray-level dependence matrix; GLRLM, gray-level run-length matrix; GLSZM, gray-level size zone matrix; NGTDM, neighborhood gray tone difference matrix.

Table 3 Comparison of BISAP and MRSI Scores Between Two Groups

| | NSAP (n=157) | SAP (n=31) | P value |
|-------------|--------------|------------|---------------------|
| BISAP score | 1 (1–2) | 2 (1–2) | 0.017 ^a |
| MRSI score | 4 (2–6) | 8 (6–8) | <0.001 ^a |

Notes: ^aData are expressed as median (interquartile range). Group comparisons were performed using the Mann–Whitney *U*-test. *P* < 0.05 was considered statistically significant.

Abbreviations: NSAP, non-severe acute pancreatitis; SAP, severe acute pancreatitis; BISAP, bedside index for severity in acute pancreatitis; MRSI, magnetic resonance severity index.

Table 4 Performance of the Five Models in the Training and Test Sets

| | Model | AUC (95% CI) | Specificity | Accuracy | Sensitivity |
|--------------|-----------------|---------------------|-------------|----------|-------------|
| | Combined model | 0.97 (0.936–1) | 0.972 | 0.954 | 0.864 |
| | Radiomics model | 0.903 (0.845–0.961) | 0.872 | 0.847 | 0.727 |
| Training set | Clinical model | 0.66 (0.55–0.77) | 0.651 | 0.634 | 0.545 |
| | BISAP model | 0.62 (0.504–0.736) | 0.578 | 0.588 | 0.636 |
| | MRSI model | 0.804 (0.714–0.894) | 0.725 | 0.748 | 0.864 |
| | Combined model | 0.979 (0.947–1) | 0.854 | 0.877 | 0.857 |
| | Radiomics model | 0.831 (0.723–0.939) | 0.75 | 0.772 | 0.889 |
| Test set | Clinical model | 0.743 (0.59–0.896) | 0.75 | 0.702 | 0.444 |
| | BISAP model | 0.668 (0.51–0.826) | 0.667 | 0.649 | 0.556 |
| | MRSI model | 0.731 (0.537–0.926) | 0.75 | 0.754 | 0.778 |

Abbreviations: AUC, area under the curve; BISAP, bedside index for severity in acute pancreatitis; MRSI, magnetic resonance severity index.

the early identification of SAP in the context of MetS, therefore supporting timely interventions such as anti-inflammatory therapies or nutritional support.

Previous investigations have addressed the prediction of AP severity.^{21–23} Qi et al developed a clinical-radiomics model using CT and clinical data, achieving an AUC of 0.905, which was lower than this study reported.²³ This study employed MRI, which avoids ionizing radiation. In particular, the T2WI sequence is highly sensitive to fluid and subtle peripancreatic inflammatory changes. Lin et al constructed a nomogram incorporating multiple laboratory indicators to predict the severity of the initial episode of hyperlipidemic AP, reporting an AUC of 0.95.²² However, their model did not directly reflect pancreatic changes. Similarly, Yi et al proposed a nomogram to predict severe hyperlipidemic AP using a combination of clinical parameters, with an AUC of 0.96, but it failed to capture alterations in pancreatic structure or function.²¹ On the other hand, this study specifically focused on AP severity prediction in patients with MetS, addressing a gap in previous research that primarily investigated the association between AP severity and MetS components through clinical data alone.⁸ Given the rising incidence of both MetS and AP and the compounding effect of MetS on AP severity, the combined model established herein demonstrated better predictive capability by incorporating both imaging and clinical variables in the MetS population.

While the BISAP and MRSI scoring systems are commonly applied to guide clinical decision-making, both exhibit inherent limitations in clinical practice. The BISAP score does not reflect localized pathological changes in the pancreas, which may result in an underestimation of SAP risk during the early disease phase. Although the MRSI score evaluates pancreatic necrosis and inflammatory extent through imaging, its dependence on qualitative assessment introduces subjectivity and limits its sensitivity to early-stage pathological changes.

Radiomics, by extracting high-dimensional quantitative features from imaging data, facilitates a shift from traditional subjective image interpretation toward objective analysis. This approach allows deeper exploration of imaging information that is not readily discernible by visual inspection.²⁴ In this study, seven radiomics features were selected, comprising one second-order feature, four higher-order features, and two features derived from wavelet transformations. The second-order feature reflects spatial distribution by assessing inter-pixel relationships within the image, capturing patterns with similar intensities or spatial arrangements. Higher-order features quantify the intrinsic textural complexity of images, such as the number of consecutive runs of pixels with identical intensities along specific directions or deviations of pixel intensities from the mean intensity of their neighborhoods. These features provide insights into the spatial heterogeneity and structural complexity of pancreatic lesions.¹⁷ Wavelet transform, a multi-resolution spatial and time frequency analysis method, applies high-pass (H) and low-pass (L) filters to decompose image signals into four sub-bands: diagonal detail (HH frequency channel), vertical detail (HL frequency channel), horizontal detail (LH frequency channel), and approximation (LL frequency channel).²⁴ This decomposition facilitates the separation of high-frequency components from low-frequency trends across multiple scales and orientations, therefore allowing the detection of subtle textural heterogeneity and edge features within pancreatic tissue. Such multi-scale analysis contributes to the identification of microstructural alterations associated with inflammation or necrosis in AP.

Among the seven selected radiomics features, the variable with the highest absolute coefficient was wavelet-HLH_glszm_GrayLevelNonUniformity. This feature is derived from the gray-level size zone matrix (GLSZM), which quantifies the size and intensity of connected voxel regions sharing the same gray level.²⁵ The GrayLevelNonUniformity metric specifically reflects the degree of gray-level variability across these regions, with higher values indicating greater heterogeneity in voxel intensities within the ROI. The prominence of this feature suggests that pancreatic tissue affected by AP may display significant gray-level non-uniformity due to inflammatory infiltration, tissue edema, or necrosis, supporting its relevance in characterizing severe pathological changes.

This study also found that patients with SAP were more likely to present with pleural effusion and ascites, which is consistent with previous findings.^{21,26} These complications primarily arise from extensive systemic inflammation and increased capillary permeability. In SAP, pancreatic necrosis and inflammatory cytokines induce a systemic inflammatory response, leading to widespread vascular endothelial dysfunction and protein-rich fluid leakage into the thoracic and abdominal cavities.^{21,26,27} The formation of pleural effusion and ascites not only complicates the clinical course but also adversely affects prognosis by contributing to respiratory compromise, prolonged hospitalization, and elevated mortality risk.^{27,28}

Among the laboratory indicators assessed, serum levels of LDL-C, HDL-C, CRP, calcium, and amylase differed significantly between groups, reflecting disparities in disease severity and systemic inflammation. Reduced LDL-C levels in SAP patients may result from the inhibitory effects of inflammatory cytokines on hepatic LDL-C synthesis or from increased vascular permeability promoting extravascular redistribution of lipoproteins.⁵ Previous research has associated lower LDL-C and HDL-C levels with persistent organ failure, increased mortality, and extended hospitalization.⁵ CRP, a widely recognized acute-phase protein, was significantly elevated in the SAP group, indicating a more pronounced systemic inflammatory response and greater tissue injury.²⁹ As a non-specific inflammatory marker, CRP is routinely applied for diagnosis, prognosis, therapeutic monitoring, and mortality prediction in inflammatory conditions.²¹ Serum amylase is widely used in the early diagnosis of AP; however, previous studies indicate that its levels do not correlate with disease severity.³⁰ In this study, amylase concentrations were raised in the SAP group relative to the NSAP group, potentially due to sampling variability or selection bias, given the limited cohort size. Larger-scale studies are warranted to confirm these findings.

Further analysis identified serum calcium levels and length of hospital stay as independent predictors of the occurrence of SAP in patients with MetS. Multiple studies have confirmed that serum calcium concentration serves as a reliable indicator for assessing the severity of AP.^{22,23,31} The underlying mechanism primarily involves autodigestive injury to pancreatic tissue during AP, wherein pancreatic lipase leaks into adjacent tissues due to necrosis or inflammation. This enzyme hydrolyzes triglycerides in surrounding adipose tissue, producing FFAs.³² The FFAs then enter the circulation and bind to calcium ions to form insoluble calcium soaps, reducing serum calcium levels and resulting in hypocalcemia.²² This phenomenon is particularly evident in SAP, where extensive pancreatic necrosis drives increased FFAs production, resulting in a higher incidence and severity of hypocalcemia. Moreover, prolonged hospitalization correlates closely with the progression of AP severity.^{33,34} As the condition advances, patients frequently develop multi-organ dysfunction and complications requiring more complex treatment regimens, thus extending the duration of hospitalization and recovery time. Surgical intervention or intensive care support is often necessary in SAP, further contributing to prolonged hospital stays.⁴

The improved predictive performance of the combined model developed in this study may be attributed to three principal factors. First, all imaging data were acquired using the same MRI scanner model under identical scanning protocols, eliminating variability caused by differing acquisition parameters. This uniformity improved the reproducibility and reliability of feature extraction.³⁵ Second, feature selection was performed sequentially using the select K-best method and the LASSO algorithm, which effectively eliminated redundant features while prioritizing those with high relevance, reliability, relevance, and accuracy. LASSO regression is particularly suitable for high-dimensional datasets and small sample sizes, allowing for the identification of features most closely associated with disease severity.^{36,37} Third, the random forest algorithm employed for model construction is an ensemble learning method that generates multiple decision trees and uses majority voting for prediction. This approach offers robust generalization ability and minimizes overfitting, resulting in reliable predictive performance.³⁸ Accordingly, the random forest-based combined model demonstrated high accuracy and stability, providing a novel predictive tool to assess SAP risk in patients with MetS.

Several limitations are associated with this study. First, as data were obtained from a single center, external validation is lacking. Future studies should incorporate multi-center cohorts to evaluate the universal applicability and robustness of the model. Second, radiomics analysis was conducted exclusively using T2WI, potentially limiting the capture of disease-relevant features from other MRI sequences. However, the application of ultra-long TR scanning technology produced images with a higher signal-to-noise ratio, partially compensating for this limitation. Finally, the number of severe cases was relatively low ($n = 31$), which may reflect the lower incidence of severe cases. Expanding the sample size is essential to increase the reliability and statistical power of the findings. Future research should integrate additional MRI sequences and larger, multi-center cohorts to construct more comprehensive and universally applicable predictive models.

Conclusion

In conclusion, this study employed radiomics features extracted from T2WI MRI sequences to characterize differences in pancreatic tissue heterogeneity between NSAP and SAP in patients with MetS. The combined model outperformed the four comparator models in predicting AP severity, demonstrating significant potential for risk assessment in this

population. This predictive approach may support clinicians in formulating personalized treatment strategies and refining clinical decision-making, ultimately contributing to an improvement in clinical outcome.

Abbreviation

SAP, severe acute pancreatitis; MetS, metabolic syndrome; AP, acute pancreatitis; BISAP, bedside index for severity in acute pancreatitis; MRSI, magnetic resonance severity index; LASSO, least absolute shrinkage and selection operator; AUC, area under the curve; DCA, decision curve analysis; BMI, body mass index; FFA, free fatty acid; MAP, mild acute pancreatitis; MSAP, moderately severe acute pancreatitis; NSAP, non-severe acute pancreatitis; CRP, C-reactive protein; LDL-C, lipoprotein cholesterol; HDL-C, high-density lipoprotein cholesterol; TR, repetition time; ROI, region of interest; ICC, intraclass correlation coefficient; ROC, receiver operating characteristic; GLSZM, gray-level size zone matrix.

Data Sharing Statement

The datasets generated/analyzed during the present study are available from the corresponding authors on reasonable request.

Ethical Statement

This study conforms to the Declaration of Helsinki, as revised in 2013, and other relevant regulations. The ethical approval was granted by the Medical Ethics Committee of Affiliated of North Sichuan Medical College [Approval number: 2024ER94-1]. The need for patient consent to review their medical records was waived by the Medical Ethics Committee of Affiliated of North Sichuan Medical College. The waiver was granted based on the following reasons: (1) The retrospective nature of the study; (2) The lack of intervention administration to patients; (3) The minimal risk posed to patients; (4) The absence of adverse impact on patient rights and health, and (5) The unequivocal assurance that patient data confidentiality would be rigorously safeguarded throughout the research process. To ensure the confidentiality of patient data, all personal identifiers have been anonymized and eliminated from the dataset.

Author Contributions

All authors made a significant contribution to the work reported, whether that is in the conception, study design, execution, acquisition of data, analysis and interpretation, or in all these areas; took part in drafting, revising or critically reviewing the article; gave final approval of the version to be published; have agreed on the journal to which the article has been submitted; and agree to be accountable for all aspects of the work.

Funding

This study has received funding from the Natural Science Foundation of Sichuan Province (2024NSFSC1775).

Disclosure

The authors report no conflicts of interest in this work.

References

1. Zhao Y, Wei J, Xiao B, et al. Early prediction of acute pancreatitis severity based on changes in pancreatic and peripancreatic computed tomography radiomics nomogram. *Quant Imaging Med Surg.* 2023;13(3):1927–1936. doi:10.21037/qims-22-821
2. Szatmary P, Grammatikopoulos T, Cai W, et al. Acute Pancreatitis: diagnosis and Treatment. *Drugs.* 2022;82(12):1251–1276. doi:10.1007/s40265-022-01766-4
3. Boxhoorn L, Voermans RP, Bouwense SA, et al. Acute pancreatitis. *Lancet.* 2020;396(10252):726–734. doi:10.1016/S0140-6736(20)31310-6
4. Trikudanathan G, Wolbrink DRJ, van Santvoort HC, Mallery S, Freeman M, Besselink MG. Current concepts in severe acute and necrotizing pancreatitis: an evidence-based approach. *Gastroenterology.* 2019;156(7):1994–2007. doi:10.1053/j.gastro.2019.01.269
5. Zhou X, Jin S, Pan J, et al. Relationship between cholesterol-related lipids and severe acute pancreatitis: from bench to bedside. *J Clin Med.* 2023;12(5):1729. doi:10.3390/jcm12051729
6. Nagy A, Juhasz MF, Gorbe A, et al. Glucose levels show independent and dose-dependent association with worsening acute pancreatitis outcomes: post-hoc analysis of a prospective, international cohort of 2250 acute pancreatitis cases. *Pancreatology.* 2021;21(7):1237–1246. doi:10.1016/j.pan.2021.06.003

7. Bai Y, Gong G, Aierken R, et al. A retrospective study investigating the clinical significance of body mass index in acute pancreatitis. *PeerJ*. 2024;12:e16854. doi:10.7717/peerj.16854
8. Niknam R, Moradi J, Jahanshahi KA, Mahmoudi L, Ejtehad F. Association between metabolic syndrome and its components with severity of acute pancreatitis. *Diabetes Metab Syndr Obes*. 2020;13:1289–1296. doi:10.2147/DMSO.S249128
9. Mikolasevic I, Milic S, Orlic L, et al. Metabolic syndrome and acute pancreatitis. *Eur J Intern Med*. 2016;32:79–83. doi:10.1016/j.ejim.2016.04.004
10. Bovolini A, Garcia J, Andrade MA, Duarte JA. Metabolic syndrome pathophysiology and predisposing factors. *Int J Sports Med*. 2021;42(3):199–214. doi:10.1055/a-1263-0898
11. Quan Y, Yang X. Metabolic syndrome and acute pancreatitis: current status and future prospects. *World J Gastroenterol*. 2024;30(45):4859–4863. doi:10.3748/wjg.v30.i45.4859
12. Zhu J, Wu L, Wang Y, Fang M, Liu Q, Zhang X. Predictive value of the Ranson and BISAP scoring systems for the severity and prognosis of acute pancreatitis: a systematic review and meta-analysis. *PLoS One*. 2024;19(4):e0302046. doi:10.1371/journal.pone.0302046
13. Tang W, Zhang XM, Xiao B, et al. Magnetic resonance imaging versus acute physiology and chronic healthy evaluation II score in predicting the severity of acute pancreatitis. *Eur J Radiol*. 2011;80(3):637–642. doi:10.1016/j.ejrad.2010.08.020
14. Liu Z, Tian L, Sun X, et al. Development and validation of a risk prediction score for the severity of acute hypertriglyceridemic pancreatitis in Chinese patients. *World J Gastroenterol*. 2022;28(33):4846–4860. doi:10.3748/wjg.v28.i33.4846
15. Jiang Z, Xiao B, Zhang X, Xu H. Early-phase vascular involvement is associated with acute pancreatitis severity: a magnetic resonance imaging study. *Quant Imaging Med Surg*. 2021;11(5):1909–1920. doi:10.21037/qims-20-280
16. Zhou T, Chen Y, Wu J, et al. Extrapaneatic inflammation on magnetic resonance imaging for the early prediction of acute pancreatitis severity. *Pancreas*. 2020;49(1):46–52. doi:10.1097/MPA.0000000000001425
17. Mayerhoefer ME, Materka A, Langs G, et al. Introduction to radiomics. *J Nucl Med*. 2020;61(4):488–495. doi:10.2967/jnumed.118.222893
18. Banks PA, Bollen TL, Dervenis C, et al. Classification of acute pancreatitis—2012: revision of the Atlanta classification and definitions by international consensus. *Gut*. 2013;62(1):102–111. doi:10.1136/gutjnl-2012-302779
19. Alberti KGMM, Eckel RH, Grundy SM, et al. Harmonizing the metabolic syndrome: a joint interim statement of the International Diabetes Federation Task Force on Epidemiology and Prevention; National Heart, Lung, and Blood Institute; American Heart Association; World Heart Federation; International Atherosclerosis Society; and International Association for the Study of Obesity. *Circulation*. 2009;120(16):1640–1645. doi:10.1161/CIRCULATIONAHA.109.192644
20. Fu Z, Zhao Z, Liang Y, et al. Impact of metabolic syndrome components on clinical outcomes in hypertriglyceridemia-induced acute pancreatitis. *World J Gastroenterol*. 2024;30(35):3996–4010. doi:10.3748/wjg.v30.i35.3996
21. Shuanglian Y, Huiling Z, Xunting L, et al. Establishment and validation of early prediction model for hypertriglyceridemic severe acute pancreatitis. *Lipids Health Dis*. 2023;22(1):218. doi:10.1186/s12944-023-01984-z
22. Lin Y, Liu Y, Lin Q, et al. Development and validation of a nomogram for predicting the severity of the first episode of hyperlipidemic acute pancreatitis. *J Inflamm Res*. 2024;17:3211–3223. doi:10.2147/JIR.S459258
23. Qi M, Lu C, Dai R, Zhang J, Hu H, Shan X. Prediction of acute pancreatitis severity based on early CT radiomics. *BMC Med Imaging*. 2024;24(1):321. doi:10.1186/s12880-024-01509-9
24. Abbasian Ardakani A, Bureau NJ, Ciaccio EJ, Acharya UR. Interpretation of radiomics features—A pictorial review. *Comput Methods Programs Biomed*. 2022;215:106609. doi:10.1016/j.cmpb.2021.106609
25. Scapicchio C, Gabelloni M, Barucci A, Cioni D, Saba L, Neri E. A deep look into radiomics. *Radiol Med*. 2021;126(10):1296–1311. doi:10.1007/s11547-021-01389-x
26. Luiken I, Eisenmann S, Garbe J, et al. Pleuropulmonary pathologies in the early phase of acute pancreatitis correlate with disease severity. *PLoS One*. 2022;17(2):e0263739. doi:10.1371/journal.pone.0263739
27. Samanta J, Rana A, Dhaka N, et al. Ascites in acute pancreatitis: not a silent bystander. *Pancreatol*. 2019;19(5):646–652. doi:10.1016/j.pan.2019.06.004
28. Zeng T, An J, Wu Y, et al. Incidence and prognostic role of pleural effusion in patients with acute pancreatitis: a meta-analysis. *Ann Med*. 2023;55(2):2285909. doi:10.1080/07853890.2023.2285909
29. Gao N, Yan C, Zhang G. Changes of serum procalcitonin (PCT), C-reactive protein (CRP), interleukin-17 (IL-17), interleukin-6 (IL-6), high mobility group protein-B1 (HMGB1) and D-dimer in patients with severe acute pancreatitis treated with continuous renal replacement therapy (CRRT) and its clinical significance. *Med Sci Monit*. 2018;24:5881–5886. doi:10.12659/MSM.910099
30. Lankisch PG, Burchard-Reckert S, Lehnick D. Underestimation of acute pancreatitis: patients with only a small increase in amylase/lipase levels can also have or develop severe acute pancreatitis. *Gut*. 1999;44(4):542–544. doi:10.1136/gut.44.4.542
31. Dong J, Shen Y, Wang Z, et al. Prediction of severe hypertriglyceridemia-associated acute pancreatitis using a nomogram based on CT findings and blood biomarkers. *Medicine*. 2024;103(17):e37911. doi:10.1097/MD.00000000000037911
32. Bashir B, Ferdousi M, Durrington P, Soran H. Pancreatic and cardiometabolic complications of severe hypertriglyceridaemia. *Curr Opin Lipidol*. 2024;35(4):208–218. doi:10.1097/MOL.0000000000000939
33. Wu B, Yang J, Dai Y, Xiong L. Combination of the BISAP score and miR-155 is applied in predicting the severity of acute pancreatitis. *Int J Gen Med*. 2022;15:7467–7474. doi:10.2147/IJGM.S384068
34. Ratiu I, Bende R, Nica C, et al. Prediction models of severity in acute biliary pancreatitis. *Diagnostics*. 2025;15(2).
35. Yamashita R, Perrin T, Chakraborty J, et al. Radiomic feature reproducibility in contrast-enhanced CT of the pancreas is affected by variabilities in scan parameters and manual segmentation. *Eur Radiol*. 2020;30(1):195–205. doi:10.1007/s00330-019-06381-8
36. Xie Y, Shi H, Han B. Bioinformatic analysis of underlying mechanisms of Kawasaki disease via weighted gene correlation network analysis (WGCNA) and the least absolute shrinkage and selection operator method (LASSO) regression model. *BMC Pediatr*. 2023;23(1):90. doi:10.1186/s12887-023-03896-4
37. Li Y, Lu F, Yin Y. Applying logistic LASSO regression for the diagnosis of atypical Crohn's disease. *Sci Rep*. 2022;12(1):11340. doi:10.1038/s41598-022-15609-5
38. Kim Y, Kim J, Kim S, Youn H, Choi J, Seo K. Machine learning-based risk prediction model for canine myxomatous mitral valve disease using electronic health record data. *Front Vet Sci*. 2023;10:1189157. doi:10.3389/fvets.2023.1189157

Journal of Inflammation Research

Publish your work in this journal

The Journal of Inflammation Research is an international, peer-reviewed open-access journal that welcomes laboratory and clinical findings on the molecular basis, cell biology and pharmacology of inflammation including original research, reviews, symposium reports, hypothesis formation and commentaries on: acute/chronic inflammation; mediators of inflammation; cellular processes; molecular mechanisms; pharmacology and novel anti-inflammatory drugs; clinical conditions involving inflammation. The manuscript management system is completely online and includes a very quick and fair peer-review system. Visit <http://www.dovepress.com/testimonials.php> to read real quotes from published authors.

Submit your manuscript here: <https://www.dovepress.com/journal-of-inflammation-research-journal>

Dovepress
Taylor & Francis Group